Alignment performance comparison between MFR and MDCO for a TMA optical system

Hyukmo Kang, Eunsong Oh, Sug-Whan Kim

Hyukmo Kang, Eunsong Oh, Sug-Whan Kim, "Alignment performance comparison between MFR and MDCO for a TMA optical system," Proc. SPIE 9582, Optical System Alignment, Tolerancing, and Verification IX, 95820G (3 September 2015); doi: 10.1117/12.2188244

SPIE.

Event: SPIE Optical Engineering + Applications, 2015, San Diego, California, United States

Alignment performance comparison between MFR and MDCO for a TMA optical system

Hyukmo Kang[a*], Eunsong Oh[a,b], Sangwon Hyun[c], Geon-Hee Kim[c], and Sug-Whan Kim[a]

[a]Space Optics Laboratory, Dept. of Astronomy, Yonsei University, Korea, Republic of
[b]Korea Ocean Satellite Center, Korea Institute of Ocean Science & Technology, Korea, Republic of
[c]Center for Analytical Instrumentation Development, Korea Basic Science Institute, Korea, Republic of

ABSTRACT

In this study, we performed alignment state estimation simulations and compared the performance of two Computer Aided Alignment (hereafter CAA) algorithms i.e. 'Merit Function Regression (MFR)' and 'Multiple Design Configuration Optimization (MDCO)' for a TMA optical system. The former minimizes the merit function using multi-field wavefront error measurements from single configuration, while the latter minimizes the merit function using single-field measured wavefront error from multiple configurations. The optical system used is an unobscured three-mirror anastigmat (TMA) optical system of 70mm in diameter, and F/5.0. It is designed for an unmanned aerial vehicle for coastal water remote sensing. The TMA consists of two aspherical mirrors, a spherical mirror and a flat folding mirror. Based on the sensitivity analysis, we set the tilt x, y of tertiary mirror as a compensator, and not considered decenter of tertiary mirror because of its spherical characteristic. For the simulation, we introduced Gaussian distribution of initial misalignment to M3. It has the mean value of zero and standard deviation of 0.5 mrad. The initial simulation result of alignment state estimation shows that both algorithms can meet the alignment requirement, λ/10 RMS WFE at 633nm. However, when we includes measurement noise, the simulation result of MFR shows greater standard deviation in RMS WFE than that of MDCO. As for the measurement, the MDCO requires single on-axis field while the MFR requires multiple fields, we concluded that the MDCO is more practical method to align the off-axis TMA optics than MFR.

Keywords: Computer-aided alignment, remote sensing, three-mirror anastigmat, error analysis, MFR, MDCO

1. INTRODUCTION

For the purpose of coastal water remote sensing, airborne or space borne sensors have been developed to overcome limited observing area of the in-situ measurement [1-3]. Though these sensors enjoy advantage of wide observing range, the time and spatial resolution are not enough to study the dynamic change of sedimentary topography of local area, ecology of tidal flats, environment of coral reefs, and etc [4-6]. Therefore, Korea Ocean Satellite Center (KOSC) is developing a push broom type hyperspectral sensor to be onboard small unmanned aerial vehicle (UAV) to complement deficiencies of previous coastal water remote sensors. This sensor is required to have high spatial resolution and signal to noise ratio, but to be compact and lightweight. To meet principle operational requirements, the fore-optics of this sensor is designed as an off-axis three mirror anastigmat (TMA) optical system [7]. We note off-axis TMA system is difficult to align precisely through trial and error approach because optical elements are not located on the same axis [8]. Therefore, computer aided alignment (CAA) algorithm is required for efficient precision alignment of the off-axis TMA. There have been many studies of CAA algorithms to align off-axis TMA using the relation between wavefront error and alignment states [8-11].

In this paper, we choose merit function regression (MFR) and multiple design configuration optimization (MDCO) method [12, 13] among aforementioned CAA algorithms, and compared performance of each algorithm. These algorithms are based on merit function, and use damped least square method to minimize its merit function value. We performed alignment state estimation simulation, and identified whether the algorithm works well under wavefront measurement noise as well. In chapter 2, we introduce the target TMA optics, and CAA algorithms are summarized briefly in chapter 3. Simulation conditions and results are reported in chapter 4 and conclusion in chapter 5.

*hyukmo@galaxy.yonsei.ac.kr

Optical System Alignment, Tolerancing, and Verification IX, edited by José Sasián, Richard N. Youngworth
Proc. of SPIE Vol. 9582, 95820G · © 2015 SPIE · CCC code: 0277-786X/15/$18 · doi: 10.1117/12.2188244

2. TMA OPTICS

The unobscured off-axis TMA optics consists of a concave aspherical primary mirror (M1), a convex aspherical secondary mirror (M2), a concave spherical tertiary mirror (M3) and a flat folding mirror (FM) (See Table 1, Figure 1(a)). The designed optical MTF value is about 0.9 at Nyquist frequency. It satisfies the requirement, over 0.75 (Figure 1(b)). The optical system has 3.3 degree of field of view, and the alignment requirement is under 0.1λ in RMS wavefront error at the center field. As mirrors are fabricated recently and each mirror meets the surface figure requirement (Figure 2), we perform CAA algorithm simulation to prepare the alignment methodology of TMA optical system.

Table 1. Specifications of off-axis TMA optics and alignment tolerance requirement [7].

Surface	Radius of curvature	Conic constant	Thickness (mm)	Semi-Diameter (mm)	Alignment Tolerance	
M1	-739.056	-4.710	-139.25	45	-	
M2 (Stop)	-237.912	-0.766	139.25	25	Decenter	0.05 mm
					Tilt	0.3 mrad
M3	-362.108	-	-125.00	40	Tilt	0.1 mrad
FM	-	-	166.02	22	Decenter	0.2 mm
					Tilt	0.7 mrad

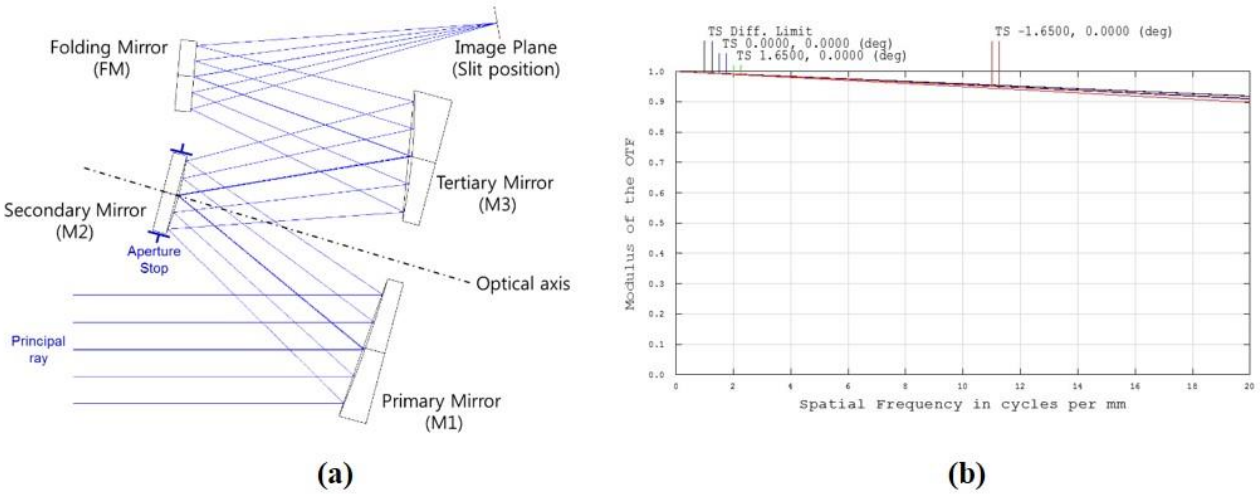

Figure 1. (a) The layout of TMA optics system (b) Optical MTF estimation value of TMA optics (@ 660nm) [7].

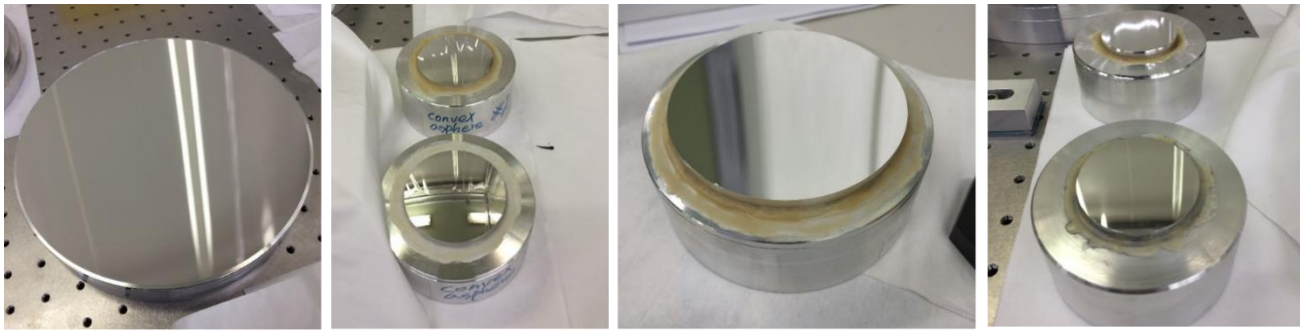

(a) (b) (c) (d)

Figure 2. Pictures of fabricated mirrors. (a) Primary mirror (one of black circles) (b) Secondary mirror (c) Tertiary mirror (d) Flat mirror

3. ALIGNMENT ALGORITHMS

3.1. Merit Function Regression method [12]

Merit function regression (MFR) method uses merit function defined as Equation 1. It consists of two Zernike coefficients sets, target (T_i) and variable (V_i), and weight factor (W_i). T_i is a set of Zernike coefficients measured from multiple fields of misaligned optical system. The V_i is also a Zernike coefficient set which represents estimated alignment state of optical system. By damped least square method, the optical design program varies V_i set to minimizes the MF value. When the MF value approaches to the minimum, the corresponding alignment parameters of V_i mean the current misaligned state.

$$\boldsymbol{MF^2} = \frac{\sum_{i=1}^{n} \boldsymbol{W_i}(\boldsymbol{V_i}-\boldsymbol{T_i})^2}{\sum \boldsymbol{W_i}} \quad (1)$$

3.2. Multiple Design Configuration Optimization method [13]

Multiple design configuration optimization (MDCO) method also uses the merit function expressed in Equation 2, but the way of acquiring merit function components is different from that of MFR. For the MDCO, we deliberately perturb the alignment element of optical system and measure the wavefront error from single on-axis field to obtain the target Zernike coefficient set, T_{ijk}. In other words, we intentionally move an i^{th} optical element about j direction with known quantity, k, and measures the wavefront error at the perturbed states. After measurement, we move the perturbed optical element back where it is initially located. This process forms one configuration, and is repeated for several times to form multiple configuration. The variable set $V_{ijk,}$ is the Zernike coefficient which corresponds to i, j, k states of T_{ijk}. Likewise the MFR, the optical design program varies V_{ijk} using damped least square method to minimize the MF value, and the corresponding alignment parameters mean the current alignment state.

$$\boldsymbol{MF^2} = \frac{\sum_{i=1}^{n}\sum_{j=1}^{m}\sum_{k=1}^{l} \boldsymbol{W_{ijk}}(\boldsymbol{V_{ijk}}-\boldsymbol{T_{ijk}})^2}{\sum \boldsymbol{W}} \quad (2)$$

4. ALIGNMENT SIMULATION

We performed Monte Carlo simulation to identify whether two algorithm can meet the aforementioned alignment requirement. In the simulation, we introduced linear and angular misalignment about x-axis and y-axis to M2, and angular misalignment to M3 about x-axis and y-axis. As we regard the position of M1 as the reference coordinate of system, we

do not consider the misalignment of M1. The position of flat mirror was not involved in this simulation as it affects little on to the performance of system. We decided to use tilt X and tilt Y of M3 as compensator based on the result of sensitivity analysis [7].

4.1. Case Definition

The simulation was performed for two error cases. In the case 1, we only considered misalignment of the compensator. We introduce misalignment to M3 as Gaussian distribution that the mean value is 0 (means designed position) and standard deviation is 0.5 mrad (means 5 times of alignment tolerance). For the case 2, we added wavefront measurement noise to the case 1 condition, and investigated how the measurement noise affects the algorithm performance. The noise included Zernike coefficients, Z_{error}, are derived from Gaussian distribution that the mean value is ideally measured Zernike coefficient, Z_{ideal} and the standard deviation is 0.25 times of Z_{ideal}. These error cases are summarized in Table 2.

We compose merit function using four sets of Zernike polynomial coefficients represent Coma (Z5, Z6) and Astigmatism (Z7, Z8). For the MFR, Zernike coefficients are sampled at the central field and two edge fields, (x, y) = (0°, 0°), (1.65°, 0°), (-1.65°, 0°). For the MDCO, on the other hand, we fixed the field at center, (x, y) = (0°, 0°), and sampled Zernike coefficients from nine configurations. Each configuration consists of initial state (current misaligned state), and deliberately moved states of M3 about tilt x, y direction with ±0.01° from initial state.

Table 2. Summary of case conditions

	Misalignment of mirror	**Wavefront measurement noise**
Case 1	Amount of misalignment of M3: $N(0, \sigma_{M3}^2), \sigma_{M3} = 0.5\ mrad$	(Not considered in Case 1)
Case 2		$Z_{error} = N(Z_{ideal}, \sigma_m^2), \sigma_m = 0.25 * Z_{ideal}$

4.2. Simulation results

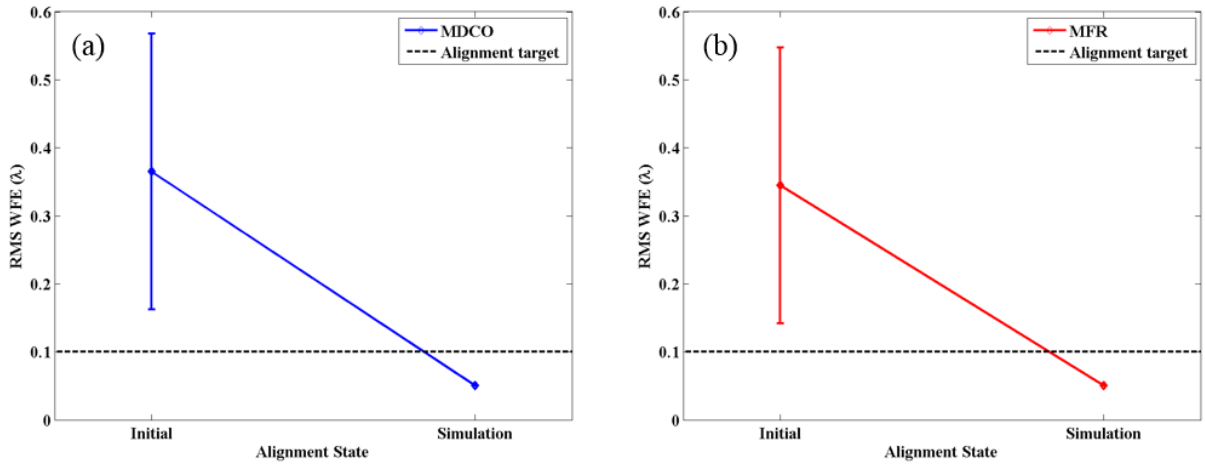

Figure 3. Results of case 1 of each algorithm. (a) MFR (b) MDCO

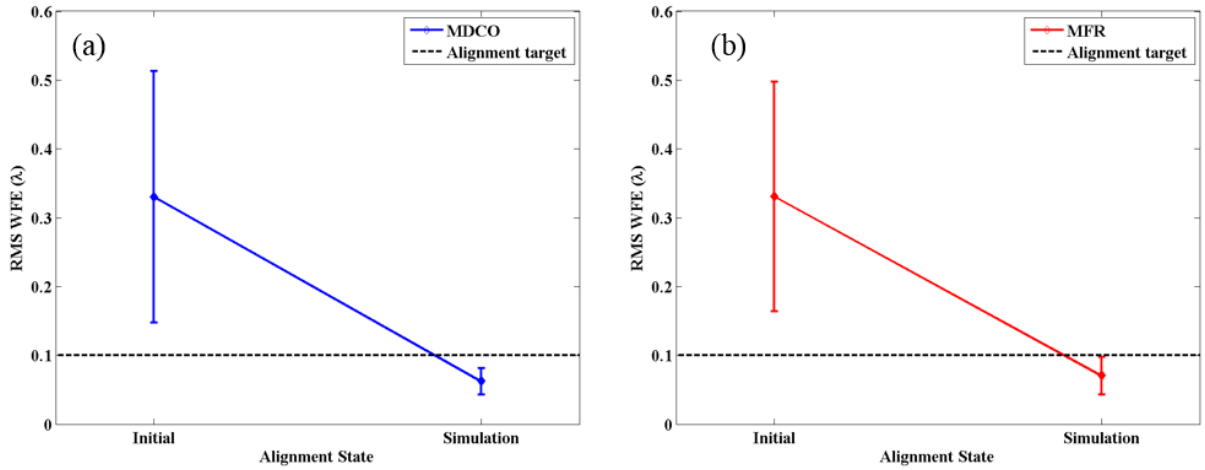

Figure 4. Results of case 2 of each algorithm. (a) MFR (b) MDCO

For the first case study, we performed 100 Monte Carlo simulation runs. Figure 3 shows the result of case 1 that both CAA algorithms meet alignment target after simulation, and have nearly zero standard deviations. This result means that both algorithms worked well when we do not consider additional error sources. For the case 2, we added wavefront measurement error to the case 1 and performed 100 Monte Carlo simulation runs. Figure 4 shows the result of the case 2, and the result mean value of both algorithms meet alignment target after simulation. However, contrary to the previous case, the standard deviation of MFR (0.0274λ) is greater than that of MDCO (0.0195λ). This result means that the MFR is more sensitive to the wavefront measurement noise than the MDCO.

5. CONCLUSION

In this study, we performed alignment state estimation simulation for an off-axis TMA optical system with two CAA algorithm, MFR and MDCO. Furthermore, we investigated influence of wavefront measurement noise and found that the MDCO method is less influenced by the wavefront measurement noise. Considering the MDCO uses single on-axis field while the MFR requires for multiple fields, we concluded that the MDCO is more practical method to align the off-axis TMA optics than MFR.

In the actual experiment, there would be more error sources that tend to degrade the performance of algorithms, such as transfer uncertainty of micrometer and surface figure error. Also, in the case of MDCO, the motion control quantity can affect the alignment state estimation performance. We plan to perform additional error analysis including transfer uncertainty, surface figure error, and align the TMA optical system in the near future.

ACKNOWLEDGMENT

This research was a part of the project titled “Development of EO/IR optical system and remote sensing technique for coastal/ocean monitoring and lunar exploration” funded by Korea Basic Science Institute.

REFERENCES

[1] G. Vane, R. O. Green, T. G. Chrien, H. T. Enmark, E. G. Ganse, and W. M. Porter, “The Airborne Visible/Infrared Imaging Spectrometer (AVIRIS),” *Remote Sens. Environ.* **44**, pp. 127–143 (1993).

[2] J.-H. Ryu, H.-J. Han, S. Cho, Y.-J. Park, and Y.-H. Ahn, "Overview of Geostationary Ocean Color Imager (GOCI) and GOCI Data Processing System (GDPS)," *Ocean Sci. J.* **47(3)**, pp. 223–233 (2012).
[3] Davis, C., Bowles, J., Leathers, R., Korwan, D., Downes, T. V., Snyder, W., Rhea, W., Chen, W., Fisher, J., et al., "Ocean PHILLS hyperspectral imager: design, characterization, and calibration," *Opt. Express* **10(4)**, 210–221 (2002).
[4] J.-H. Ryu, J.-K. Choi, and Y.-K. Lee, "Potential of remote sensing in management of tidal flats: A case study of thematic mapping in the Korean tidal flats," *Ocean & Coastal Management* **47(3)**, pp. 223–233 (2012).
[5] Choi, J., Ryu, J., Eom, J., Hoon, J., "Analysis on the seasonal variations of microphytobenthos distribution in a tidal flat using remotely sensed data," *Proc. of SPIE* **7858** (2001).
[6] Mumby, P. J., Chisholm, J. R. M., Clark, C. D., Hedley, J. D., Jaubert, J., "Spectrographic imaging: A bird's-eye view of the health of coral reefs," *Nature* **413(6851)**, pp. 36-37 (2001).
[7] Eunsong Oh, Hyukmo Kang, Sangwon Hyun, Geon-Hee Kim, YoungJe Park, Jong-Kuk Choi, S.-W. K., "Design and Performance Analysis of an Off-Axis Three-Mirror Telescope for Remote Sensing of Coastal Water," *Hankook Kwanghak Hoeji* **26**, pp. 155–161 (2015)
[8] Jeong, H. J., Lawrence, G. N., Nahm, K. B., "Auto-Alignment Of A Three-Mirror Off-Axis Telescope By Reverse Optimization And End-To-End Aberration Measurements," *Proc. of SPIE* **0818**, pp. 419–430 (1987).
[9] Figoski, J. W., Shrode, T. E.., Moore, G. F., "Computer-Aided Alignment Of A Wide-Field, Three-Mirror, Unobscured, High-Resolution Sensor," *Proc. of SPIE* **1049**, pp. 166–177 (1989).
[10] Geyl, R., "Design and fabrication of a three-mirror, flat-field anastigmat for high-resolution earth observation," *Proc. of SPIE* **2210**, pp. 739–746 (1994).
[11] Lundgren, M. A., Wolfe, W. L., "Alignment of a three-mirror off-axis telescope by reverse optimization," *Opt. Eng.* **30(3)**, 307–311 (1991).
[12] Kim, S., Yang, H.-S., Lee, Y.-W., Kim, S.-W., "Merit function regression method for efficient alignment control of two-mirror optical systems," *Opt. Express* **15(8)**, 5059–5068 (2007).
[13] Oh, E.-S., Kim, S., Kim, Y., Lee, H., Kim, S.-W., Yang, H.-S., "Integration of differential wavefront sampling with merit function regression for efficient alignment of three-mirror anastigmat optical system," *Proc. of SPIE* **7793**, 77930F (2010).